Electronic Supplementary Material (ESI) for Journal of Materials Chemistry A.

Ti-Anchored Ti_2CO_2 Monolayer (MXene) as a Single-Atom Catalyst for CO Oxidation

Xu Zhang, Jincheng Lei, Dihua Wu, Xudong Zhao, Yu Jing and Zhen Zhou*

Tianjin Key Laboratory of Metal and Molecule Based Material Chemistry, Computational Centre for Molecular Science, Institute of New Energy Material Chemistry, Collaborative Innovation Center of Chemical Science and Engineering (Tianjin), School of Materials Science and Engineering, National Institute for Advanced Materials, Nankai University, Tianjin 300350, P.R. China

Table S1. The binding energies E_b (eV) and atomic charge a.c. (|e|) of anchoring Ti at three different anchoring sites of Ti_2CO_2 monolayer.

	Ti
E_b (1)	-7.68
E_b (2)	-7.22
E_b (3)	-3.51
a.c. (1)	+1.55
a.c. (2)	+1.53
a.c. (3)	+0.96

Table S2. The diffusion barriers E (eV) of Ti on Ti_2CO_2 monolayer (Fig. S2).

	Ti
E(IS-TS1)	1.43
E(MS-TS2)	0.99

Table S3. The binding energies E_b (eV) of the second Ti on site 1.

	Ti
E_b	-2.18

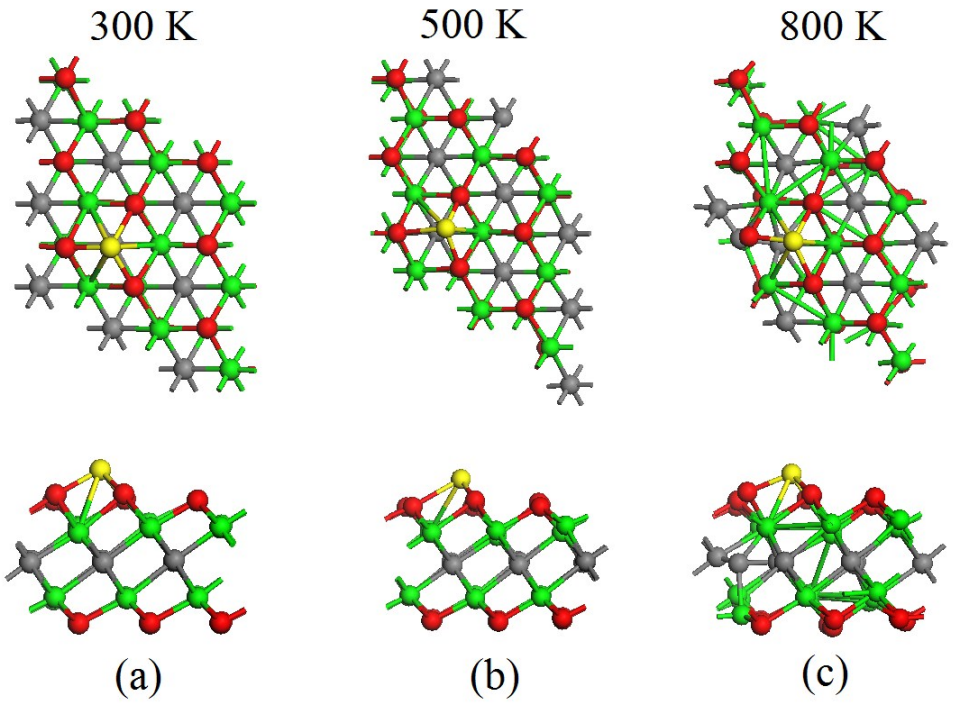

Fig. S1 A snapshot of the equilibrium structure of Ti/Ti_2CO_2 at (a) 300 K, (b) 500 K, and (c) 800 K, respectively, at the end of 5 ps first-principles molecular dynamic (MD) simulation.

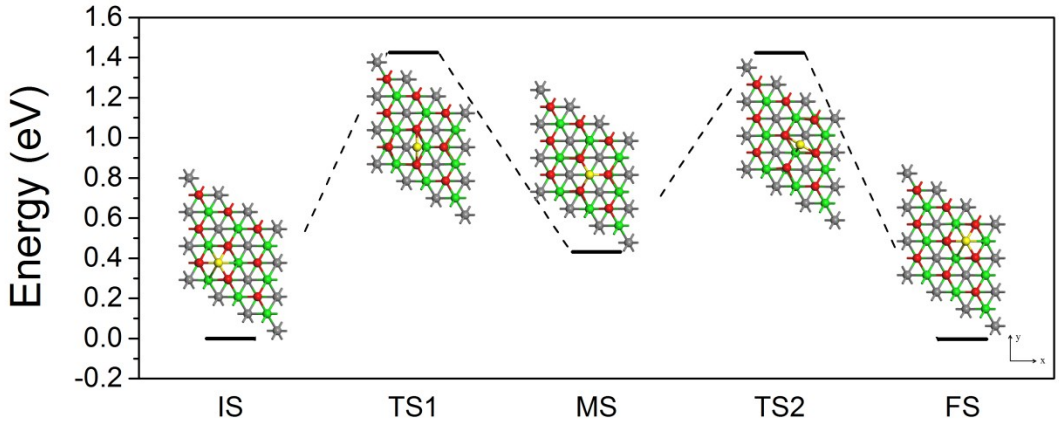

Fig. S2 Diffusion pathway of anchoring Ti on Ti_2CO_2 monolayer.

Table S4. The adsorption energies E_{ad} (eV), the atomic charge a.c. (|e|) and the bond length d (Å) of O_2 and CO on Ti-anchored Ti_2CO_2 monolayer.

	Ti
E_{ad} (O_2)	-4.83
a.c. (O_2)	-0.78
d (O_2)	1.46
E_{ad} (CO)	-1.11
a.c. (CO)	-0.22
d (CO)	1.15

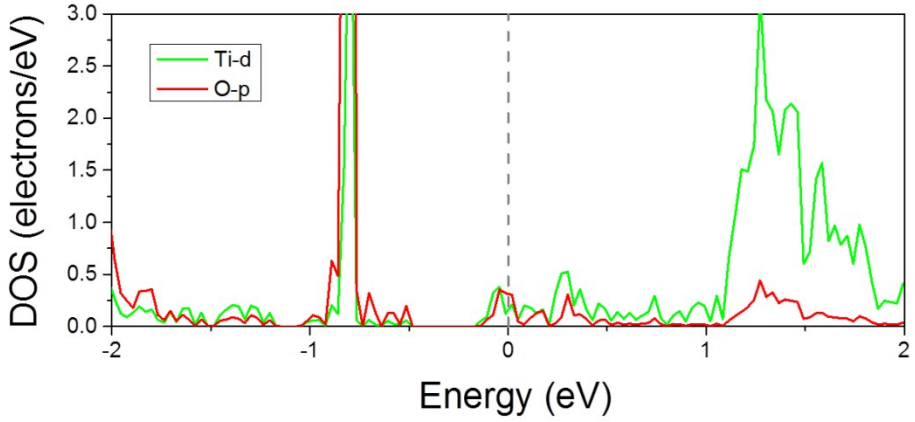

Fig. S3 Computed projected density of states (PDOS) for the p-orbital of the adsorbed O_2 molecular and the *d*-orbital of the anchored Ti.

Table S5. The bond length d (Å) of each state on Ti-anchored Ti_2CO_2 monolayer (Fig. 4).

State	Bond	Ti
IS	d(O1-O2)	1.46
TS1	d(C-O1)	2.36
	d(C-O2)	2.22
	d(O1-O2)	2.20
MS1	d(C-O1)	1.36
	d(C-O2)	1.41
	d(M-O1)	1.94
	d(M-O2)	1.86
TS2	d(C-O2)	1.99
	d(M-O1)	2.13
MS2	d(O1-O2)	3.15
TS3	d(C-O2)	1.67
FS1	d(M-O2)	2.12

Table S6. Energy barriers E (eV) and reaction energies ΔE (eV) of each state on Ti-anchored Ti_2CO_2 monolayer (Fig. 4).

	Ti
E(IS-TS1)	0.25
E(MS1-TS2)	0.37
E(MS3-TS3)	1.01
ΔE(IS-MS1)	-3.67
ΔE(MS1-MS2)	-0.03
ΔE(MS3-FS1)	-0.08

Table S7. The binding energies E_b (eV) and the atomic charge a.c. (|e|) of the O atom above the anchoring Ti.

	Ti
E_b (O)	-8.55
a.c. (O)	-0.69

.

Table S8. The bond length d (Å) of each state on Ti-anchored Ti_2CO_2 monolayer (Fig. 5).

State	Bond	Ti
TS	C1-O1	2.61
	O1-O2	2.59
FS2	O1-M	2.47
	O2-M	2.31

Table S9. Energy barriers E (eV) and reaction energies ΔE (eV) of each state on Ti-anchored Ti_2CO_2 monolayer (Fig. 5).

	Ti
E(IS-TS)	0.23
ΔE(IS-FS2)	-0.39

.

Table S10. The bond length d (Å) of each state on Ti/Cr anchored Ti_2CO_2 monolayer (Fig. 6 and Fig. S6).

State	Bond	Ti
IS	d(O1-O2)	1.49
	d(M-C)	2.16
	d(M-O2)	1.88
TS1	d(O1-O2)	1.73
	d(C-O1)	1.34
	d(M-C)	2.19
	d(M-O2)	1.81
MS1	d(O1-O2)	2.74
	d(C-O1)	1.18
	d(M-O1)	3.04
	d(M-O2)	1.67
MS2	d(C-O2)	2.41
	d(M-O2)	1.70
TS2	d(C-O2)	1.62
MS3	d(C-O2)	1.32
	d(M-O2)	1.94
TS3	d(M-O2)	2.10
FS	d(M-O2)	2.36

Table S11. Energy barriers E (eV) and reaction energies ΔE (eV) of each state on Ti/Cr anchored Ti_2CO_2 monolayer (Fig. 4 and Fig. S4).

	Ti
E(IS-TS1)	0.33
E(MS2-TS2)	0.35
E(MS3-TS3)	0.35
ΔE(IS-MS1)	-3.59
ΔE(MS2-MS3)	0.15
ΔE(MS3-FS1)	0.14

Table S12. The binding energies E_b (eV) and atomic charge a.c. (|e|) of single-metal atom M at three different anchoring sites of Ti_2CO_2 monolayer.

	Cr	Au	Co	Rh	Ru	Pd	Cu	Fe
E_b (1)	-7.72	-0.86	-4.48	-3.32	-5.10	-1.75	-2.23	-5.75
E_b (2)	-6.62	-0.34	-4.04	-2.96	-4.56	-1.81	-2.06	-4.92
E_b (3)	-3.36	-1.11	-2.89	-1.20	-2.81	-1.61	-0.69	-3.01
a.c. (1)	+1.25	+0.33	+0.71	+0.49	+0.68	+0.37	+0.78	+0.85
a.c. (2)	+1.14	+0.34	+0.85	+0.61	+0.89	+0.46	+0.78	+1.03
a.c. (3)	0.84	+0.36	+0.60	+0.44	+0.63	+0.41	+0.43	+0.69

Considering the stability of the M-anchored Ti_2CO_2, we used the structure with the highest binding energy. As shown in Table S12, the binding energy of Cr in site 1 is even higher than that of Ti and is at least ~2 eV higher than that of other atoms. Then the diffusion behavior of anchoring Cr on Ti_2CO_2 monolayer was examined and the diffusion barriers are shown in Fig. S4. The high diffusion barrier (1.86 eV) indicates it is difficult to agglomerate for Cr on Ti_2CO_2.

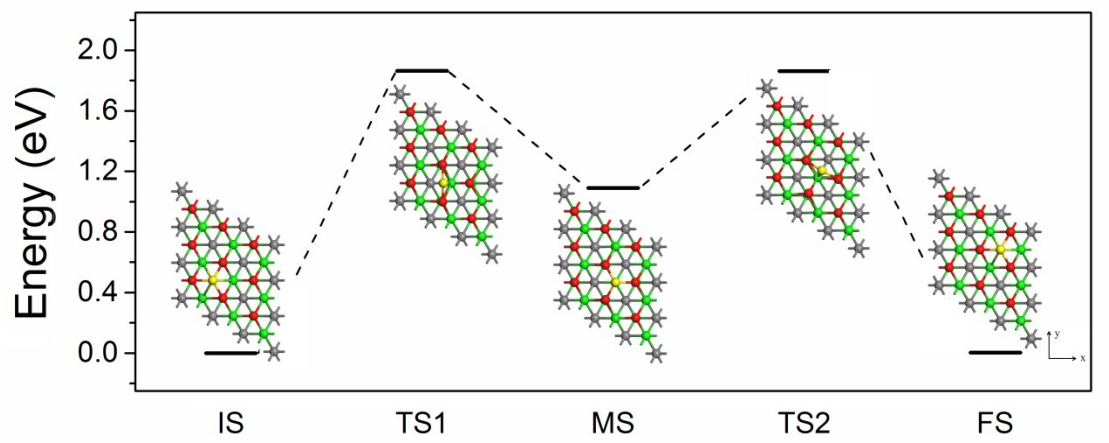

Fig. S4 Diffusion pathway of anchoring Cr on Ti_2CO_2 monolayer.

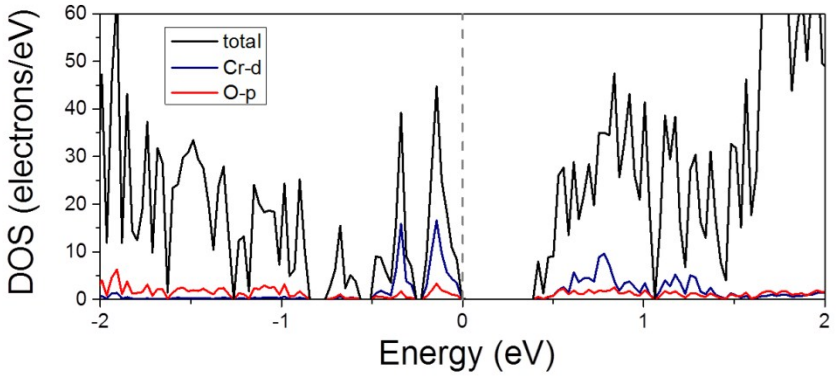

Fig. S5 Computed total density of states (TDOS) and projected density of states (PDOS) for the Cr-anchored Ti_2CO_2.

The total density of states (TDOS) and projected density of states (PDOS) for Cr-anchored Ti_2CO_2 were also calculated (Fig. S5) to investigate the interaction between the Ti_2CO_2 monolayer and the anchoring Cr. Compared with Ti atoms (Fig. 2), Cr would have less empty *d* state, thus, the interaction between anchoring Cr atoms and adsorbed O_2 or CO would be weaker.

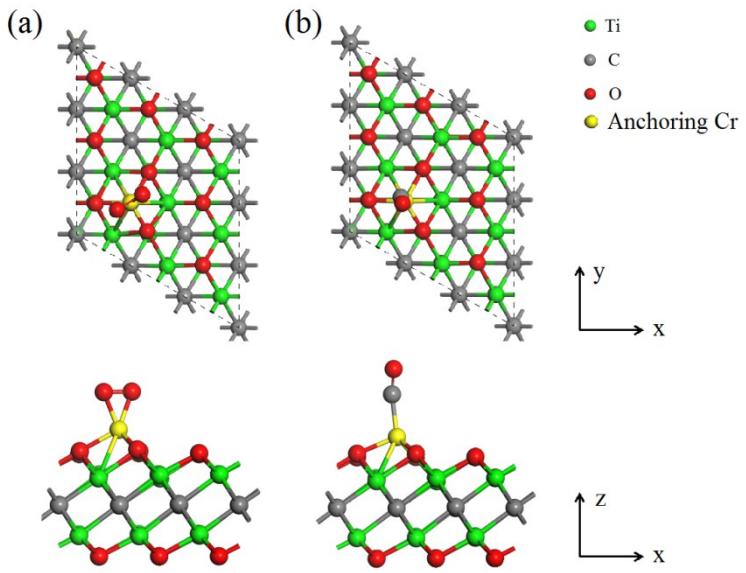

Fig. S6 Top (upper) and side (lower) view of the optimized energetically most favorable structures of (a) O_2 and (b) CO adsorbed on Cr-anchored Ti_2CO_2.

The most energetically favorable configuration for the O_2 and CO adsorption on Cr-anchored Ti_2CO_2 is shown in Fig. S6. More details are shown in Table S13. The PDOS for the *d*-orbital of Cr atoms and the *p*-orbital of adsorbed O_2 was also calculated as shown in Fig. S7.

Table S13. The adsorption energies E_{ad} (eV), the atomic charge a.c. (|e|) and the bond length d (Å) of O_2 and CO on Cr-anchored Ti_2CO_2 monolayer.

	Cr
E_{ad} (O_2)	-3.74
a.c. (O_2)	-0.61
d (O_2)	1.43
E_{ad} (CO)	-1.02
a.c. (CO)	-0.17
d (CO)	1.15

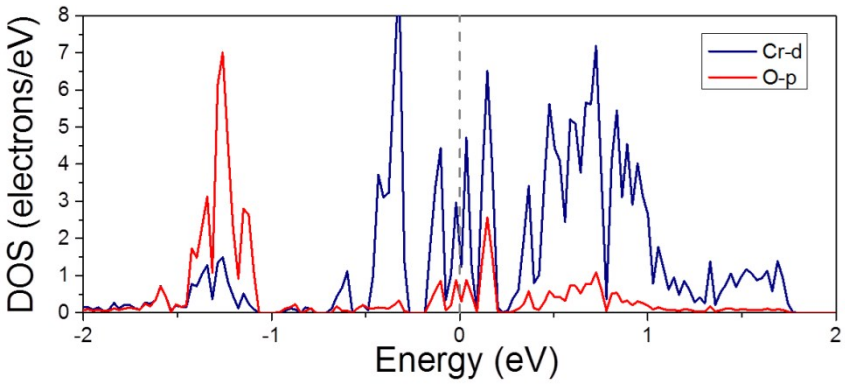

Fig. S7 Computed projected density of states (PDOS) for the *p*-orbital of the adsorbed O_2 molecular and the *d*-orbital of the anchored Cr.

The strong hybridization between the *d*-orbital of Cr atoms and the *p*-orbital of O_2 could be clearly seen from the PDOS. However, compared with Ti/Ti_2CO_2 (Table S4), the adsorption energy of O_2 and CO is lower, which is consistent with the analysis from PDOS (Fig. S5 and Fig. 2). Moreover, the bond length of O_2 adsorbed on Ti/Ti_2CO_2 is longer which could indicate that the O_2 adsorbed on Ti/Ti_2CO_2 would be more activated. To further prove the analysis, the mechanisms of CO oxidation on Cr-anchored Ti_2CO_2 were also investigated.

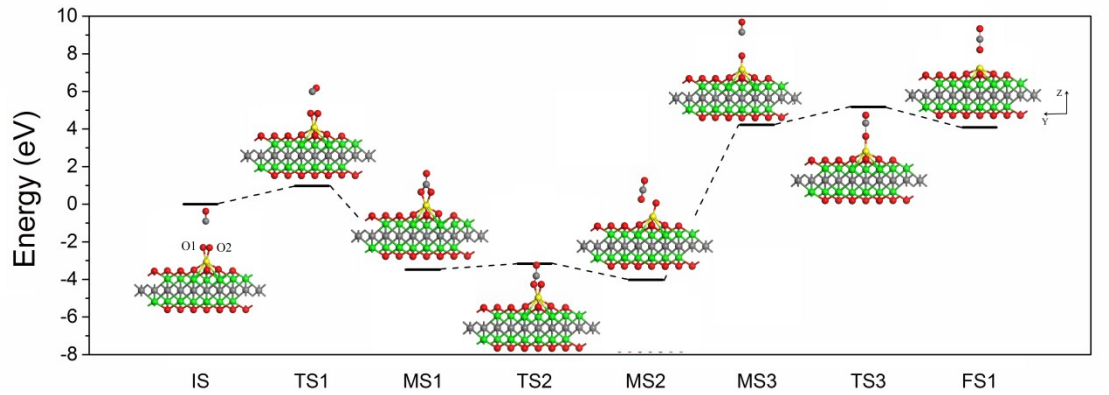

Fig. S8 The reaction path way I of CO oxidation on Cr-anchored Ti_2CO_2 monolayer via ER mechanism.

Table S14. The bond length d (Å) of each state on Cr-anchored Ti_2CO_2 monolayer (Fig. S8).

State	Bond	Cr
IS	d(O1-O2)	1.43
TS1	d(C-O1)	2.63
	d(C-O2)	2.55
	d(O1-O2)	2.15
MS1	d(C-O1)	1.37
	d(C-O2)	1.37
	d(M-O1)	1.85
	d(M-O2)	1.86
TS2	d(C-O2)	1.77
	d(M-O1)	2.10
MS2	d(O1-O2)	2.90
TS3	d(C-O2)	1.52
FS1	d(M-O2)	2.10

Table S15. Energy barriers E (eV) and reaction energies ΔE (eV) of each state on Cr-anchored Ti_2CO_2 monolayer (Fig. S8).

	Cr
E(IS-TS1)	0.97
E(MS1-TS2)	0.31
E(MS3-TS3)	1.05
ΔE(IS-MS1)	-3.48
ΔE(MS1-MS2)	-0.54
ΔE(MS3-FS1)	-0.13

Table S16. The binding energies E_b (eV) and the atomic charge a.c. (|e|) of the O atom above the anchoring Cr.

	Cr
E_b (O)	-7.80
a.c. (O)	-0.62

As shown in Table S15, the energy barriers of the first and last process are much higher than that of Ti/Ti_2CO_2, which further supports the analysis from PDOS and the bond length of the activated O_2.

Then, the ER mechanism via pathway II was also investigated as shown in Fig. S9.

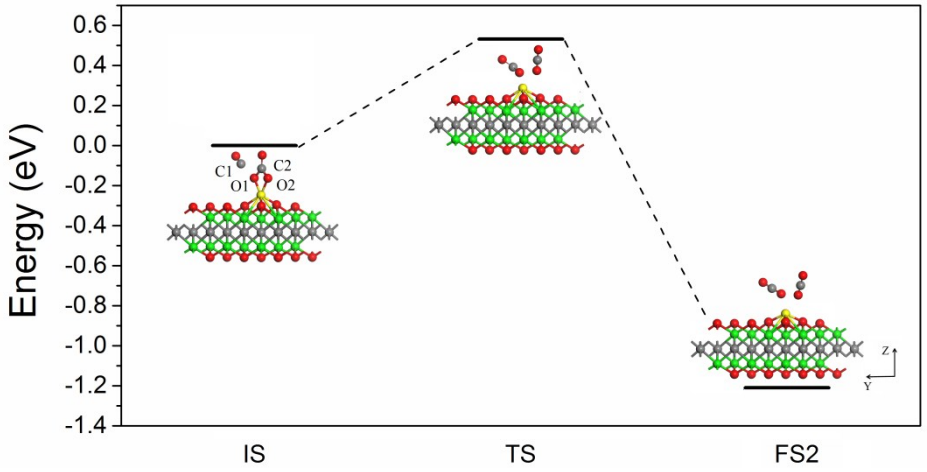

Fig. S9 Reaction pathway II of CO oxidation on Cr-anchored Ti_2CO_2 monolayer via ER mechanism.

Table S17. The bond length d (Å) of each state on Cr-anchored Ti_2CO_2 monolayer (Fig. S9).

State	Bond	Cr
TS	C1-O1	1.62
	O1-O2	2.43
FS2	O1-M	2.26
	O2-M	2.21

Table S18. Energy barriers E (eV) and reaction energies ΔE (eV) of each state on Cr-anchored Ti_2CO_2 monolayer (Fig. S9).

	Cr
E(IS-TS)	0.53
ΔE(IS-FS2)	-1.21

As shown in Table S18, the energy barrier of this process is low and exothermic. However, the energy barrier of the first process of ER mechanism is very high (0.97 eV).

Then, the LH mechanism for CO oxidation in Cr/Ti_2CO_2 was also considered as shown in Fig.S10.

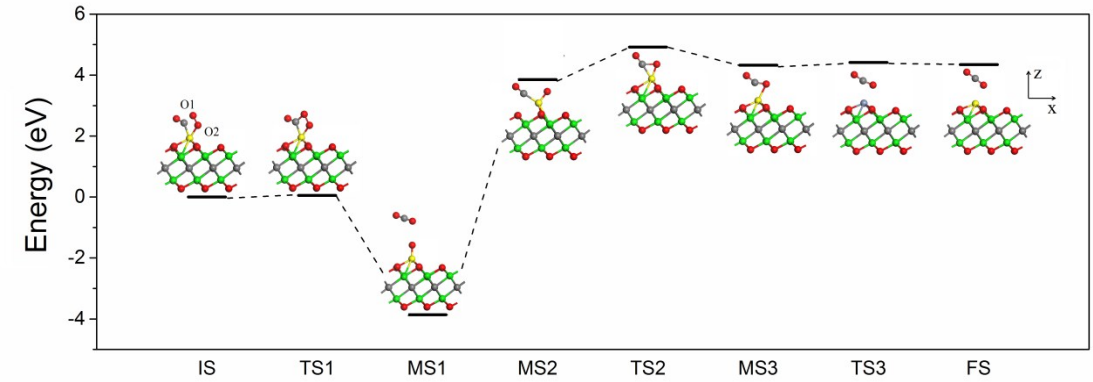

Fig. S10 The reaction path way of CO oxidation on Cr-anchored Ti_2CO_2 monolayer via LH mechanism.

Table S19. The bond length d (Å) of each state on Cr-anchored Ti_2CO_2 monolayer (Fig. S10).

State	Bond	Cr
IS	d(O1-O2)	1.50
	d(M-C)	2.05
	d(M-O2)	1.77
TS1	d(O1-O2)	1.67
	d(C-O1)	1.35
	d(M-C)	2.07
	d(M-O2)	1.70
MS1	d(O1-O2)	2.78
	d(C-O1)	1.18
	d(M-O1)	4.35
	d(M-O2)	1.64
MS2	d(C-O2)	2.59
	d(M-O2)	1.58
TS2	d(C-O2)	1.60
MS3	d(C-O2)	1.26
	d(M-O2)	2.04
TS3	d(M-O2)	2.29
FS	d(M-O2)	2.25

Table S20. Energy barriers E (eV) and reaction energies ΔE (eV) of each state on Cr-anchored Ti_2CO_2 monolayer (Fig. S10).

	Cr
E(IS-TS1)	0.08
E(MS2-TS2)	1.01
E(MS3-TS3)	0.09
ΔE(IS-MS1)	-3.86
ΔE(MS2-MS3)	0.47
ΔE(MS3-FS1)	0.01

The barrier energies of the first and last process of LH mechanism (0.08 and 0.09 eV) are almost barrierless. However, the barrier energy of the second process of LH mechanism is much higher (1.01 eV) than that of ER mechanism via path way II (0.97 and 0.53 eV). Moreover, the last two processes are thermodynamically unfavored. From the above results, Ti/Ti_2CO_2 would exhibit better performance than Cr/Ti_2CO_2 for CO oxidation. This might be caused that the Ti atoms on Ti_2CO_2 have more empty d states; therefore, the interaction with adsorbed O_2 is stronger than Cr/Ti_2CO_2. As a result, the adsorbed O_2 would be more active on Ti/Ti_2CO_2, and Ti/Ti_2CO_2 would have higher catalytic activity.

Table S21. Energy barriers E (eV) and reaction energies ΔE (eV) of each state on different single-metal atom catalysts. The bolds mean the highest energy barrier or endothermic process. / means the energies that were not given in the ref. ~ means the energies were got from Figures.

Catalysts		Reaction Process	E	ΔE	Ref
Ti/Ti_2CO_2	ER	$CO+O_2 \rightarrow CO_3$	**0.25**	-3.67	This work
		$CO_3+CO \rightarrow 2CO_2$	0.23	-0.39	
	LH	$CO+O_2 \rightarrow CO_2+O$	0.33	-3.59	
		$CO+O \rightarrow OCO$	**0.35**	**0.15**	
		$OCO \rightarrow CO_2$	**0.35**	**0.14**	
Fe/Graphene	ER	$CO+O_2 \rightarrow CO_3$	**0.58**	-3.73	[1]
		$CO_3+CO \rightarrow 2CO_2$	0.57	-1.68	
Oxygen-Defective Pt/FeO_x	LH	$CO+O_2 \rightarrow CO_2+O$	0.49	-1.98	[2]
		$CO+O \rightarrow CO_2$	**0.79**	-0.20	
Oxygen-Defective Rh/FeO_x	LH	$CO+O_2 \rightarrow CO_2+O$	0.43	-1.5	
		$CO+O \rightarrow OCO$	0.00	-1.23	
		$OCO \rightarrow CO_2$	**0.53**	**0.44**	
Oxygen-Defective Pd/FeO_x	LH	$CO+O_2 \rightarrow CO_2+O$	0.53	-2.26	
		$CO+O \rightarrow OCO$	**0.57**	-0.35	
		$OCO \rightarrow CO_2$	0.55	**0.17**	
Oxygen-Defective Ru/FeO_x	LH	$CO+O_2 \rightarrow CO_2+O$	0.27	-0.99	[3]
		$CO+O \rightarrow OCO$	**0.79**	**0.44**	
		$OCO \rightarrow CO_2$	0.12	**0.09**	
		CO_2 release	-	**0.44**	
Vacancy-Free Co/FeO_x	LH	$CO+O_2 \rightarrow OOCO$	**0.45**	-0.52	
		$OOCO \rightarrow O+CO_2$	0.00	-2.54	
		$O+CO \rightarrow CO_2$	0.00	-2.36	
Vacancy-Free Ti/FeO_x	LH	$CO+O_2 \rightarrow OOCO$	**0.37**	-0.11	
		$OOCO \rightarrow O+CO_2$	0.00	-2.40	
		$O+CO \rightarrow CO_2$	0.00	-2.24	

Vacancy-Free Ru/FeO_x	LH	$CO+O_2 \rightarrow OOCO$	0.26	-0.26	
		$OOCO \rightarrow O+CO_2$	0.00	-3.49	
		$O+CO \rightarrow CO_2$	**0.27**	-0.99	

Catalysts		Reaction Process	E	ΔE	Ref
Cu/Graphene	LH	$CO+O_2 \rightarrow OOCO$	0.25	-0.77	[4]
		$OOCO \rightarrow O+CO_2$	**0.54**	-1.79	
	ER	$O+CO \rightarrow CO_2$	0.00	-	
Pt/pri-Graphene	LH	$CO+O_2 \rightarrow CO_2+O$	**1.03**	~-1.8	
Single-Vacancy Pt/Graphene	ER	$CO+O_2 \rightarrow CO_3$	0.23	~-4.2	[5]
		$CO_3 \rightarrow CO_2+O$	**0.77**	**~0.2**	
		$CO+O \rightarrow CO_2$	0.59	~-1.0	
Fe/h-BN	LH	$CO+O_2 \rightarrow CO_2+O$	**0.58**	~3.3	[6]
	ER	$CO+O_2 \rightarrow CO_2+O$	0.56	~-4	
		$CO+O \rightarrow CO_2$	**0.61**	~-0.8	
Ru/h-BN	LH	$CO+O_2 \rightarrow OOCO$	**0.41**	**0.38**	[7]
		$OOCO \rightarrow O+CO_2$	0.39	-3.59	
		$CO+O \rightarrow COO$	0.37	-0.29	
		$COO \rightarrow CO_2$	0.28	/	
	ER	$CO+O_2 \rightarrow CO_2+O$	0.42	-4.06	
		$CO+O \rightarrow CO_2$	**0.71**	/	
Fe/Graphene Oxide	LH	$CO+O_2 \rightarrow CO_2+O$	**2.03**	-2.52	[8]
	ER	$CO+O_2 \rightarrow CO_3$	0.60	-3.47	
		$CO_3 \rightarrow O+CO$	0.86	**0.69**	
		$CO+O \rightarrow CO_2$	**0.93**	-1.88	
	ER	$CO_3+CO \rightarrow 2CO_2$	**0.70**	-1.42	
Fe/Graphyne	LH	$CO+O_2 \rightarrow CO_2+O$	**1.06**	~-3.5	[9]
	ER	$CO+O_2 \rightarrow CO_3$	0.21	-3.30	
		$CO_3 \rightarrow CO_2+O$	0.07	/	

		$CO+O \rightarrow CO_2$	**0.89**	~-0.3	

Catalysts		Reaction Process	E	ΔE	Ref
CoPc	LH	$CO+O_2 \rightarrow CO_2+O$	**0.65**	-1.75	[10]
		$CO+O \rightarrow CO_2$	0.12	-4.03	
	ER	$CO+O_2 \rightarrow CO_3$	**1.23**	-3.40	
		$CO_3 \rightarrow CO_2+O$	0.23	-0.52	
		$CO+O \rightarrow CO_2$	0.10	-4.29	
FePc		LH	**0.73**	/	
		ER	**0.85**	/	
CuPc		LH	**0.93**	/	
		ER	**0.90**	/	
ZnPc		LH	**0.51**	/	
		ER	**0.85**	/	
Au/Silicene	LH	$CO+O_2 \rightarrow OOCO$	0.28	-0.27	[11]
		$OOCO \rightarrow OOCO$	0.10	-0.18	
		$OOCO \rightarrow O+CO_2$	**0.34**	-1.97	
	ER	$O+CO \rightarrow CO_2$	**0.32**	-3.19	

(1) Li, Y.; Zhou, Z.; Yu, G.; Chen, W.; Chen, Z. *J. Phys. Chem. C* **2010**, *114*, 6250.

(2) Qiao, B.; Wang, A.; Yang, X.; Allard, L. F.; Jiang, Z.; Cui, Y.; Liu, J.; Li, J.; Zhang, T. *Nat. Chem.* **2011**, *3*, 634.

(3) Li, F.; Li, Y.; Zeng, X. C.; Chen, Z. *ACS Catal.* **2015**, *5*, 544.

(4) Song, E. H.; Wen, Z.; Jiang, Q. *J. Phys. Chem. C* **2011**, *115*, 3678.

(5) Tang, Y.; Yang, Z.; Dai, X. *Phys. Chem. Chem. Phys.* **2012**, *14*, 16566.

(6) Zhao, P.; Su, Y.; Zhang, Y.; Li, S.-J.; Chen, G. *Chem. Phys. Lett.* **2011**, *515*, 159.

(7) Huang, C.; Ye, X.; Chen, C.; Lin, S.; Xie, D. *Comput. Theor. Chem.* **2013**, *1011*, 5.

(8) Li, F.; Zhao, J.; Chen, Z. *J. Phys. Chem. C* **2012**, *116*, 2507.

(9) Wu, P.; Du, P.; Zhang, H.; Cai, C. *Phys. Chem. Chem. Phys.* **2015**, *17*, 1441.

(10) Deng, Q.; Zhao, L.; Gao, X.; Zhang, M.; Luo, Y.; Zhao, Y. *Small* **2013**, *9*, 3506.

(11) Li, C.; Yang, S.; Li, S.-S.; Xia, J.-B.; Li, J. *J. Phys. Chem. C* **2013**, *117*, 483.